NASA TECHNICAL NOTE

NASA TN D-5272

C. 1

NASA TN D-5272

AN EXPERIMENTAL AND THEORETICAL INVESTIGATION OF A SYMMETRICAL AND A CAMBERED DELTA WING CONFIGURATION AT MACH NUMBERS FROM 2.0 TO 10.7

by Walter P. Nelms, Jr., Ralph L. Carmichael, and Charles R. Castellano

Ames Research Center
Moffett Field, Calif.

NATIONAL AERONAUTICS AND SPACE ADMINISTRATION • WASHINGTON, D. C. • JUNE 1969

AN EXPERIMENTAL AND THEORETICAL INVESTIGATION OF A SYMMETRICAL AND A CAMBERED DELTA WING CONFIGURATION AT MACH NUMBERS FROM 2.0 TO 10.7

By Walter P. Nelms, Jr., Ralph L. Carmichael, and Charles R. Castellano

Ames Research Center
Moffett Field, Calif.

NATIONAL AERONAUTICS AND SPACE ADMINISTRATION

For sale by the Clearinghouse for Federal Scientific and Technical Information
Springfield, Virginia 22151 – CFSTI price $3.00

AN EXPERIMENTAL AND THEORETICAL INVESTIGATION OF A SYMMETRICAL AND A CAMBERED DELTA WING CONFIGURATION AT MACH NUMBERS FROM 2.0 TO 10.7

By Walter P. Nelms, Jr., Ralph L. Carmichael, and Charles R. Castellano

Ames Research Center

SUMMARY

An experimental and theoretical investigation has been made of the effect of wing camber on the longitudinal aerodynamic characteristics of a configuration representative of an airplane designed to cruise at hypersonic speeds. A 70° swept delta wing with a symmetrical section and 4-percent thickness ratio was compared to one of identical planform and thickness which was cambered so as to have a flat lower surface. Experimental data were obtained at eight Mach numbers, from 1.99 to 10.70, and compared with estimates from three different theoretical procedures.

The investigation indicated that a configuration with a flat-bottomed wing was in no way superior to a similar configuration with a symmetrical wing section. In fact, at the lowest Mach numbers of this study the flat-bottomed wing had a large negative pitching moment at zero lift, which would indicate fairly substantial values of trim drag. The characteristics could be predicted with a fair degree of accuracy by the tangent-wedge -- tangent-cone procedure.

INTRODUCTION

It has been shown theoretically (refs. 1, 2, 3) that at high hypersonic speeds, the airfoil section with the highest lift-drag ratio has a flat lower surface. In reference 1, a comparison was made between a symmetrical double wedge section of 4-percent thickness ratio and a flat-bottomed section with the same thickness distribution. The symmetrical section had the highest ratio of lift to drag at Mach numbers of 2 and 5, while the flat-bottomed section was superior at Mach numbers of 10 and 20. In the same study (ref. 1), large negative pitching-moment coefficients at zero lift were noted for the flat-bottomed wing at the lower Mach numbers, indicating potentially large values of trim drag for a practical configuration. In view of these results on airfoil sections, it appeared very desirable to make similar calculations on a configuration representative of an actual hypersonic airplane and to compare these predictions with experimentally determined characteristics over a wide Mach number range.

Therefore the present investigation explored the effects of camber, both experimentally and theoretically, for two simple wing-body configurations over

the Mach number range from 1.99 to 10.70. The configurations had 4-percent-thick, 70° swept delta wings, one with a symmetrical and the other a cambered airfoil section. The tests were made in air in the Ames 1- by 3-Foot Supersonic and 3.5-Foot Hypersonic Wind Tunnels. Estimates from three theories, two linearized supersonic theories and the tangent-cone -- tangent-wedge hypersonic method, have been used in a comparison with the experimental results.

SYMBOLS

The force and moment coefficients are referenced to the stability axes system with the moment reference center located on the fuselage centerline 10.962 inches (27.843 cm) from the nose. This location corresponds to the 25-percent point of the mean aerodynamic chord. The subscripts "cambered wing" and "symmetrical wing" as used herein indicate the total configuration with the respective wing.

The results in this report are presented in the U. S. Customary System of Units with equivalent values indicated parenthetically in the International System. Reference 4 presents conversion factors and physical constants for the two systems of units.

c	local chord length
$\bar{c}$	mean aerodynamic chord of wing
C_D	drag coefficient, $\frac{\text{drag}}{qS}$
C_{D_o}	drag coefficient at zero lift
ΔC_{D_o}	zero-lift drag increment $(C_{D_{o\text{cambered wing}}} - C_{D_{o\text{symmetrical wing}}})$
C_D'	$C_D - C_{D_{o\text{symmetrical wing}}}$
C_L	lift coefficient, $\frac{\text{lift}}{qS}$
C_{L_α}	lift-curve slope at zero lift
C_{L_o}	lift coefficient at zero angle of attack
C_m	pitching-moment coefficient, $\frac{\text{pitching moment}}{qS\bar{c}}$
C_{m_o}	pitching-moment coefficient at zero lift
$\frac{\partial C_m}{\partial C_L}$	slope of pitching-moment curve at zero lift
d	body diameter

d_{max}	maximum body diameter
$\frac{L}{D}$	lift-drag ratio
$\left(\frac{L}{D}\right)_{max}$	maximum lift-drag ratio
l	overall body length
M	free-stream Mach number
q	free-stream dynamic pressure
r	radial coordinate
S	wing planform area
t	maximum thickness of airfoil section
$\frac{t}{c}$	wing thickness ratio
x	longitudinal coordinate, measured rearward from model nose
x_{cg}	longitudinal distance of moment reference center from model nose
α	angle of attack (referenced to fuselage centerline)

MODEL

A drawing of the model, including a table of body coordinates, is shown in figure 1. Figure 2 presents details of the symmetrical and cambered airfoil sections for the wings that were tested. Figure 3 is a photograph of the model with the cambered wing.

The model consisted of a body which could be fitted with a wing having either a symmetrical or a cambered airfoil section. The body had a circular cross section, a fineness ratio (l/d) of 12 and a Sears-Haack profile extending back 11.133 inches (28.278 cm) from the nose. From this point aft, the external contour of the body consisted of a cone frustum.

Both wings tested had identical 70° swept-leading-edge delta planforms, aspect ratios of 1.46, and maximum thicknesses of 4 percent ($t/c = 0.04$) in the stream direction. The first wing tested (fig. 2(a)) had a symmetrical wedge-slab-wedge airfoil section with ridge lines at 30 and 70 percent of the local chords on the upper and lower surfaces. This wing was mounted in a mid-wing position on the body so that the centerline of the airfoil section coincided with the centerline of the body. The second wing (fig. 2(b)) had a cambered airfoil section with a flat lower surface and ridge lines on the upper surface at 30 and 70 percent of the local chords. The cambered wing was mounted in such a manner that a plane containing the wing lower surface passed through the centerline of the body.

TESTS

The tests were made in air in the Ames 1- by 3-Foot Supersonic and 3.5-Foot Hypersonic Wind Tunnels over a Mach number range from 1.99 to 10.70. In the 1- by 3-foot facility, the Mach number was varied from 1.99 to 4.81 and in the 3.5-foot tunnel, the Mach numbers were 5.31, 7.42, and 10.70. The following table lists the nominal stagnation temperatures and pressures, along with the resulting unit Reynolds numbers, used for the tests.

Mach number	Stagnation temperature		Stagnation pressure		Unit Reynolds number	
	^{o}F	(^{o}K)	lb/in.^{2}	(kN/m^2)	per ft	(per m)
1.99	100	(311)	29	(200)	7.2×10^6	(23.6×10^6)
2.56	114	(319)	40	(276)	7.2×10^6	(23.6×10^6)
3.14	114	(319)	53	(365)	7.1×10^6	(23.3×10^6)
4.07	108	(315)	57	(393)	4.8×10^6	(15.7×10^6)
4.81	117	(320)	59	(407)	3.5×10^6	(11.5×10^6)
5.31	790	(694)	262	(1806)	3.4×10^6	(11.2×10^6)
7.42	790	(694)	613	(4226)	3.8×10^6	(12.5×10^6)
10.70	1420	(1044)	1592	(10976)	1.8×10^6	(5.9×10^6)

The tests were conducted over a nominal angle-of-attack range from -4 to $+12^{o}$. The model was sting-mounted through the fuselage base, and force and moment measurements were made with an internally mounted six-component strain-gage balance. The angle of attack was corrected for both wind-tunnel flow misalinement and for balance and sting deflections caused by aerodynamic loads. Fuselage base pressure measurements were made and the axial-force data were adjusted to a condition corresponding to free-stream static pressure on the base.

In view of the difficulty in fixing transition at the higher Mach numbers, the entire test was conducted with no artificial induction of boundary-layer transition.

The estimated maximum errors in the various measured quantities based on repeatability of the data and known precision of the measuring equipment are as follows:

	Supersonic tests	Hypersonic tests
C_L	±0.002	±0.003
C_m	±0.0006	±0.0008
C_D	±0.0003	±0.0004
M	±0.01	±0.05
α	$\pm0.1^{o}$	$\pm0.1^{o}$

THEORETICAL METHODS

Three methods were used to predict the longitudinal aerodynamic characteristics of the symmetrical and cambered wing configurations. The first two methods have been successfully applied in previous studies at low supersonic speeds and the third is a standard method for estimating hypersonic characteristics. Each method was used for all of the Mach numbers of this report, namely 1.99 to 10.70, despite the fact that none of the procedures were expected to be applicable for this entire speed range. The calculation techniques employed in these methods, along with pertinent references, are, briefly, as follows:

Method I (ref. 5).- The wing characteristics were computed by linearized supersonic theory and the forebody lift was calculated by slender body theory. The effect of camber on the wing characteristics was computed by three elementary delta wing solutions superimposed in accordance with the techniques described in reference 6. Carry-over factors calculated by slender body theory were used to compute wing-body interference. The interference loadings induced by the wing camber on the fuselage afterbody were neglected, as were the effects of fuselage boattail.

Method II (ref. 7).- Both the wing and body characteristics were computed by a linearized supersonic theory consisting of numerical calculations by aerodynamic influence coefficients with panels located on the wing and body to account for interference effects. The pressures were computed by the linear pressure coefficient formula and the maximum number of panels allowable in the computer program described in reference 7.

Method III (ref. 3).- The wing characteristics were computed by the tangent-wedge method and the body characteristics were calculated by the tangent-cone procedure. For the expansion regions of both the wing and body, a Prandtl-Meyer expansion from free stream was employed. The computer program of reference 8 was used for the numerical computations for Method III.

RESULTS AND DISCUSSION

Presentation of Results

The longitudinal force and moment data obtained experimentally are presented in figure 4. These data are shown for Mach numbers of 1.99, 2.56, 3.14, 4.07, 4.81, 5.31, 7.42, and 10.70 at the Reynolds numbers indicated in the Tests section of this report. A comparison of the experimental data with the results obtained by the three theoretical prediction techniques is presented in figure 5 for Mach numbers from 1.99 to 10.70. Summary plots of the experimental and theoretical results as a function of Mach number are shown in figure 6.

Discussion of Experimental Results

Lift.- At the lower speeds, the lift curves for both the symmetrical and cambered wing configurations are linear for the entire angle-of-attack range of the study (fig. 4). At a Mach number of 4.81, however, a nonlinearity begins to appear in the curves resulting in increased lift-curve slope with increasing lift. This nonlinearity becomes quite significant at the higher speeds. A comparison of the slopes of the lift curves for the two configurations shows that for any given value of lift at the lower speeds, the slopes of the curves are the same. However, as the Mach number is increased, the configuration with the cambered wing exhibits the greater value of lift-curve slope at the higher lift coefficients. The magnitude of C_{L_α} obtained by experiment decreases from about 0.03 at a Mach number of 1.99 to about 0.01 at $M = 10.70$.

As would be expected at the lower supersonic speeds, the configuration with the cambered wing has a positive value of lift at zero angle of attack whereas above $M \approx 2.9$, where the wing leading edge becomes supersonic, this trend reverses.

Drag and lift-drag ratio.- The configuration with the cambered wing has a higher drag at zero lift. This difference in C_{D_o} is very significant at the lower speeds but quite insignificant at $M = 10.70$. However, the symmetrical configuration has a greater drag due to lift and, as a net result of these contrasting effects, the maximum lift-to-drag ratio for the two configurations is virtually the same at all Mach numbers of this study. The experimental results indicate values of $(L/D)_{max}$ decreasing from 5.7 at a Mach number of 1.99 to about 3.3 at the highest Mach number of 10.70.

Pitching moment.- At the lower Mach numbers, the configuration with the cambered wing exhibits a relatively high negative pitching-moment coefficient at zero lift (fig. 4). This value is reduced to zero or becomes slightly positive at the higher speeds. The slopes of the pitching-moment curves at zero lift for both the symmetrical and cambered wing configurations are nearly identical and show decreasing stability with increasing Mach number. This stability change represents a forward movement of the aerodynamic center from 45 percent of the mean aerodynamic chord at $M = 1.99$ to about 15 percent of the mean aerodynamic chord at $M = 10.70$. This large forward aerodynamic center travel with increasing Mach number is due primarily to the increased forebody loading at the hypersonic speeds. At the higher Mach numbers and higher lift coefficients, the configuration with the cambered wing is slightly more stable.

Except for the larger C_{D_o} and more negative C_{m_o} of the cambered wing configuration at the lower speeds, the two models have similar longitudinal aerodynamic characteristics for the conditions of these tests. Thus the overall longitudinal aerodynamic performance of this configuration is essentially unaffected by wing camber at the higher hypersonic speeds of this study.

Comparison With Theory

Lift.- At the lower Mach numbers, the lift-curve slope and lift at zero angle of attack as predicted by the linear theory of Method I agree well with the experimental results obtained for both the symmetrical and cambered wing configurations (figs. 5 and 6(a)). This good agreement at the lower speeds is maintained for the entire angle-of-attack range of this study. In the Mach number range of 4.07 to 5.31, Method I gives good estimates of C_{L_α} but tends to underpredict the lift-curve slope at the higher lift coefficients since the theory does not account for the nonlinearities that appear in the experimental results. Above $M = 5.31$, Method I shows fair agreement with the experimental lift-curve slopes near zero lift, but badly underestimates this parameter at the higher angles of attack. Likewise, at the higher speeds, Method I does not predict the negative C_{L_0} values associated with the cambered wing configuration. It can be concluded then, that Method I gives good estimates of the lift characteristics for these configurations for Mach numbers up to 4.07. The departure from experiment above this Mach number would probably be expected, since this is a linear theory procedure and generally out of its range of applicability.

As can be seen in figures 5(a) and 6(a), the linearized supersonic theory of Method II gives good estimates of the lift-curve slopes for both configurations at Mach number 1.99. However, at $M = 2.56$ and 3.14 this theoretical procedure tends to overestimate the lift-curve slopes but the estimates agree well with the experimental values of lift at zero angle of attack. For the higher Mach numbers, the lift predictions of Method II are similar to those of Method I. At the lower speeds, however, Method I tends to give better overall lift estimates than those of Method II.

At a Mach number of 1.99, the hypersonic theory of Method III tends to overpredict the lift-curve slopes for both configurations and to underestimate the difference in the magnitude of the lift between the two wings (figs. 5 and 6(a)). However, at most of the remaining Mach numbers of this study, the estimates of C_{L_α} by Method III show fair to good agreement with the experimental results. Because of nonlinearities in the prediction of pressure coefficient with increasing angle of attack, the lift curves as computed by this procedure exhibit increasing slope with increasing lift. Consequently, at the lower Mach numbers and higher lift coefficients, the estimated lift curves have a greater slope than the experimental results. At the higher speeds, however, the nonlinear lift curves predicted by this method exhibit fair to good agreement with the experimental data. In contrast to the other two theories, Method III predicts a negative value of C_{L_0} for the cambered wing at the higher Mach numbers. In view of the prediction of nonlinear characteristics throughout the Mach number range of this study, Method III generally gives the best overall results of the three analytical procedures used in this investigation.

Drag.- The experimental and theoretical drag characteristics of the symmetrical and cambered wing configurations are compared in figures 5 and 6(a). The results are presented so as to show the drag differences between the two configurations rather than the overall drag level. The parameter

C_D' of figure 5 represents the drag coefficient less the C_{D_o} of the symmetrical wing configuration. In figure 6(a), the increments in zero-lift drag between the symmetrical and cambered wing configurations are presented as a function of Mach number.

The linear theory of Method I tends to overpredict the C_{D_o} increment between the configurations at the lowest two Mach numbers of 1.99 and 2.56; the results are better at the higher speeds. At M = 1.99, Method I agrees well with the experimental drag polar of the symmetrical wing configuration but tends to underestimate the drag due to lift of the configuration with the cambered wing. For M = 2.56 and 3.14, Method I slightly underpredicts the drag due to lift for both configurations at the highest values of lift. At Mach numbers of 7.42 and 10.70, Method I tends to predict a greater drag due to lift for both winged configurations at the higher values of lift than shown in the experimental data.

Except for a slight overprediction at M = 2, the linearized supersonic theory of Method II gives good estimates of the zero-lift drag differences between the two configurations for the entire speed range of the study. In general, the drag due to lift of both configurations at the higher values of lift is underpredicted by Method II at M = 1.99 to 5.31. For M = 7.42 and 10.70, Method II overpredicts the drag due to lift at the higher values of lift, but shows good results similar to those of Method I at the lower values.

As was the case with Method II, the tangent-cone -- tangent-wedge procedure of Method III gives good estimates of the increments in zero-lift drag between the symmetrical and cambered wing configurations throughout the Mach number range considered. At most Mach numbers of the study, Method III generally underpredicts the drag due to lift characteristics for both configurations at the higher values of lift, whereas, with exception of Mach number 1.99, it gives good results at the medium and low values of lift. It can be concluded, then, that theoretical Methods II and III give the best overall predictions of the differences in C_{D_o} between the configurations while none of the methods is superior as far as drag due to lift estimates are concerned.

Pitching moment.- Figures 5 and 6(b) present a comparison of the experimental and theoretical pitching-moment characteristics of the symmetrical and cambered wing configurations. At M = 1.99, theoretical Method I gives good estimates of the slopes of the pitching-moment curves at zero lift, but tends to overpredict the stability of both configurations for Mach numbers 2.56 through 7.42. The good agreement that occurs at M = 10.70 between the theoretical and experimental stability curves is probably only fortuitous. With the exception of the good results at Mach numbers 2.56 through 4.07, Method I tends to predict a slightly greater negative C_{m_o} than is exhibited by the experimental data for the Mach number range of the study.

The supersonic linearized theory of Method II tends to predict much more stability for both configurations than the experimental results

indicate. The aerodynamic center locations as estimated by this theory are from about 11 to 14 percent of the mean aerodynamic chord rearward of the experimental data at M = 3.14 and 10.70, respectively. In addition, for the Mach number range considered, Method II predicts a much larger negative C_{m_o} than is obtained from the experimental tests of the cambered wing configuration. Except at the lowest Mach number, it appears that neither Method I nor II adequately estimates the longitudinal pressure distribution for these configurations.

The $\partial C_m/\partial C_L$ values predicted by the tangent-cone -- tangent-wedge theory of Method III show from fair to good agreement with the experimental values for M = 1.99 through 7.42, but at M = 10.70 this theory tends to underestimate the stability. At the higher Mach numbers, the slight differences in stability of these configurations at zero lift, as indicated by this theory, do not appear in the experimental data. Method III predicts C_{m_o} to be less negative than the experimental values for M = 1.99 to 3.14, but this theoretical technique gives good estimates at all the higher speeds for this same parameter. Of the three theoretical procedures considered in this study, Method III gives the best overall results for both $\partial C_m/\partial C_L$ and C_{m_o}.

CONCLUSIONS

An experimental and theoretical investigation has been made of the effect of wing camber on the longitudinal aerodynamic characteristics of a configuration representative of an airplane designed to cruise at hypersonic speeds. A 70° delta wing with symmetrical section and 4-percent thickness ratio was compared to one of identical planform and thickness which was cambered so as to have a flat lower surface. Experimental data were obtained at eight Mach numbers, from 1.99 to 10.70, and compared with estimates from three different theoretical procedures. The following results were obtained:

1. There was no significant difference in maximum lift-to-drag ratio between the two wings at any of the Mach numbers of this study.

2. At the lowest Mach numbers, the cambered wing produced a very large negative pitching moment at zero lift. However, at the higher hypersonic speeds, the pitching-moment characteristics of this configuration were essentially unaffected by wing camber.

3. None of the three theoretical procedures yielded results that could be said to agree well with the experiment in all cases. This might be expected, since the methods were at times used outside the Mach number range of their applicability. However, the best overall results for this configuration were obtained by Method III, which is a tangent-wedge -- tangent-cone approximation procedure.

4. The large differences in zero lift drag, C_{D_o}, predicted by the theoretical methods at M = 1.99 are actually observed in the experiment.

These penalties in C_{D_o} associated with the cambered wing were offset by the higher drag due to lift of the symmetrical wing.

Ames Research Center
National Aeronautics and Space Administration
Moffett Field, Calif., 94035, Mar. 17, 1969
126-13-03-01-00-21

REFERENCES

1. Linnell, Richard D.: Two-Dimensional Airfoils in Hypersonic Flows. J. Aero. Sci., vol. 16, no. 1, Jan. 1949, pp. 22-30.

2. Truitt, R. W.: Hypersonic Aerodynamics. Ronald Press, New York, 1959, p. 54.

3. Cox, R. N.; and Crabtree, L. F.: Elements of Hypersonic Aerodynamics. Academic Press, New York, 1965.

4. Mechtly, E. A.: The International System of Units; Physical Constants and Conversion Factors. NASA SP-7012, 1964.

5. Pitts, William C.; Nielsen, Jack N.; and Kaattari, George E.: Lift and Center of Pressure of Wing-Body-Tail Combinations at Subsonic, Transonic, and Supersonic Speeds. NACA Rept. 1307, 1957.

6. Cohen, D.: Formulas for the Supersonic Loading, Lift, and Drag of Flat Swept-Back Wings With Leading Edges Behind the Mach Lines. NACA Rept. 1050, 1951.

7. Woodward, F. A.; Tinoco, E. N.; and Larsen, J. W.: Analysis and Design of Supersonic Wing-Body Combinations, Including Flow Properties in the Near Field, Part I: Theory and Application. NASA CR-73106, 1967.

8. Gentry, Arvel E.: Hypersonic Arbitrary-Body Aerodynamic Computer Program. Vols. I and II. Douglas Rept. DAC 56080, June 1967.

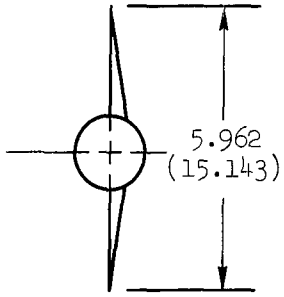

BODY COORDINATES

x/l	d/d_{max}	x/l	d/d_{max}
0.0	0.0	0.3250	0.9070
0.0025	0.0316	0.3500	0.9326
0.0050	0.0532	0.3750	0.9528
0.0100	0.0889	0.4000	0.9703
0.0150	0.1200	0.4250	0.9832
0.0250	0.1745	0.4500	0.9926
0.0500	0.2877	0.4750	0.9986
0.0750	0.3827	0.5000	1.0000
0.1000	0.4650	0.5250	0.9986
0.1250	0.5384	0.5500	0.9926
0.1500	0.6038	0.5750	0.9832
0.1750	0.6624	0.6000	0.9703
0.2000	0.7156	0.6250	0.9535
0.2250	0.7635	0.7298	0.8753
0.2500	0.8059	0.7965	0.8255
0.2750	0.8443	0.9193	0.7345
0.3000	0.8774	1.0000	0.6739

d_{max} = 1.484 (3.769)

l = 17.813 (45.245)

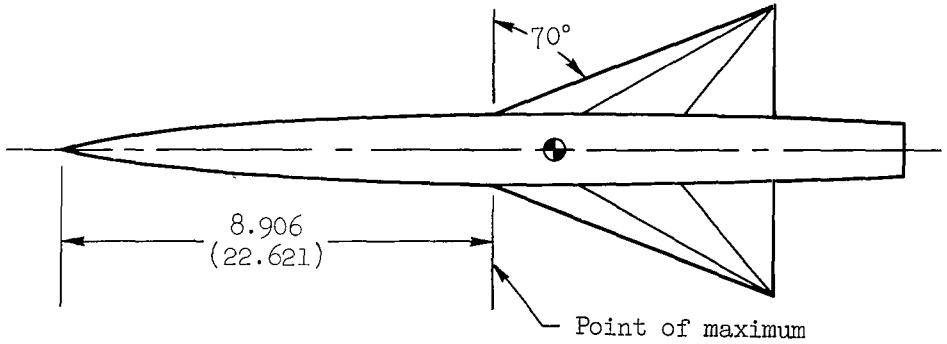

Note: All dimensions are in inches (cm)

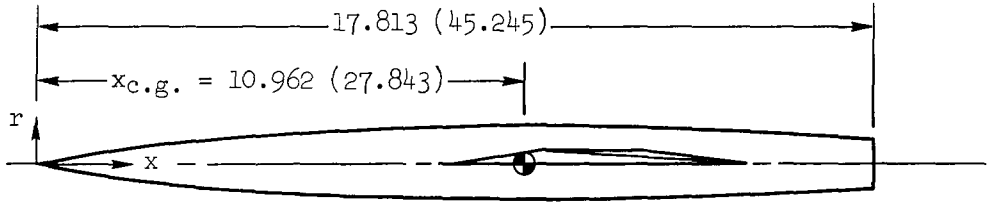

S = 24.414 sq in. (140.625 sq cm)

$\bar{c}$ = 5.463 (31.467)

Figure 1.- Model drawing; cambered wing shown.

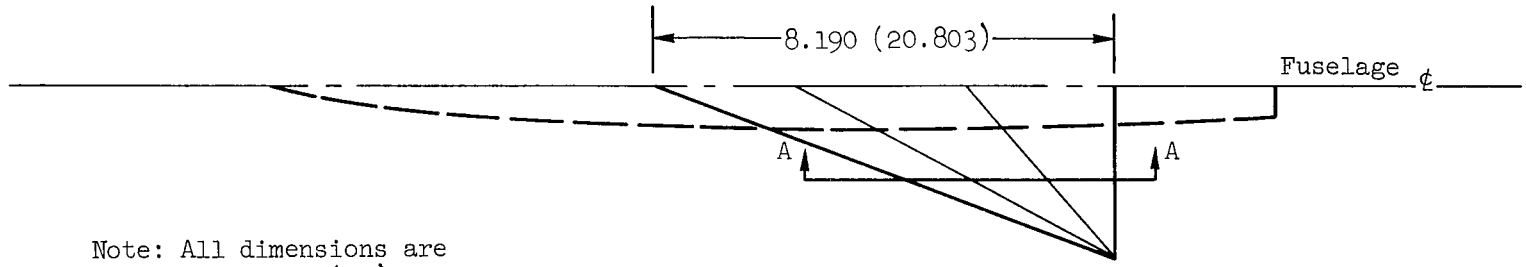

Note: All dimensions are in inches (cm)

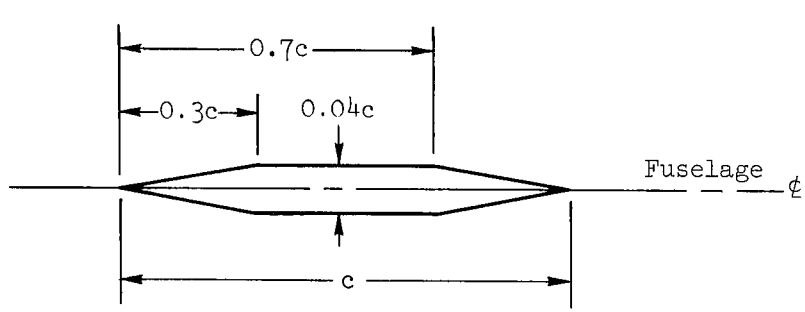

(a) Section A-A of symmetrical wing (Not to scale)

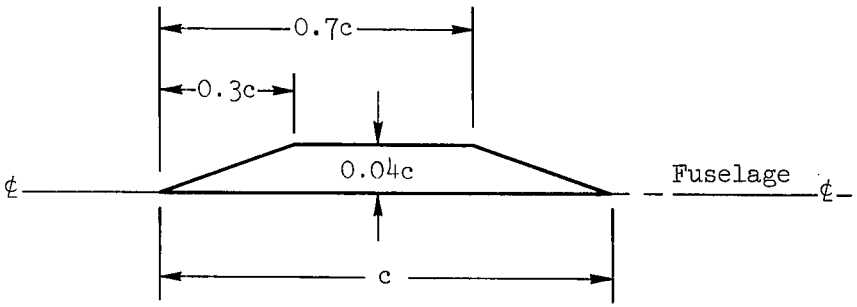

(b) Section A-A of cambered wing (Not to scale)

Figure 2.- Details of symmetrical and cambered wings.

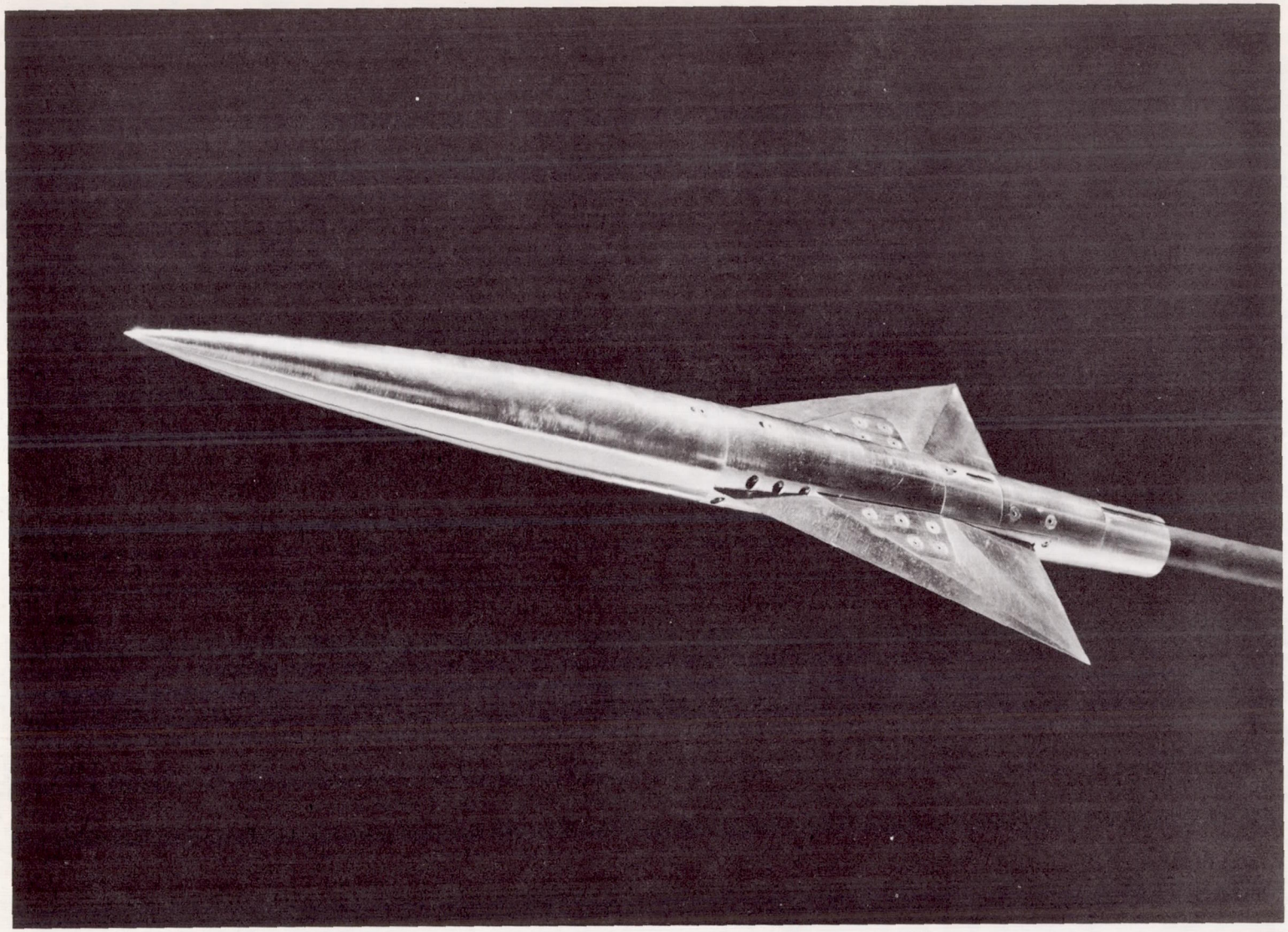

A-37263

Figure 3.- Model with cambered wing.

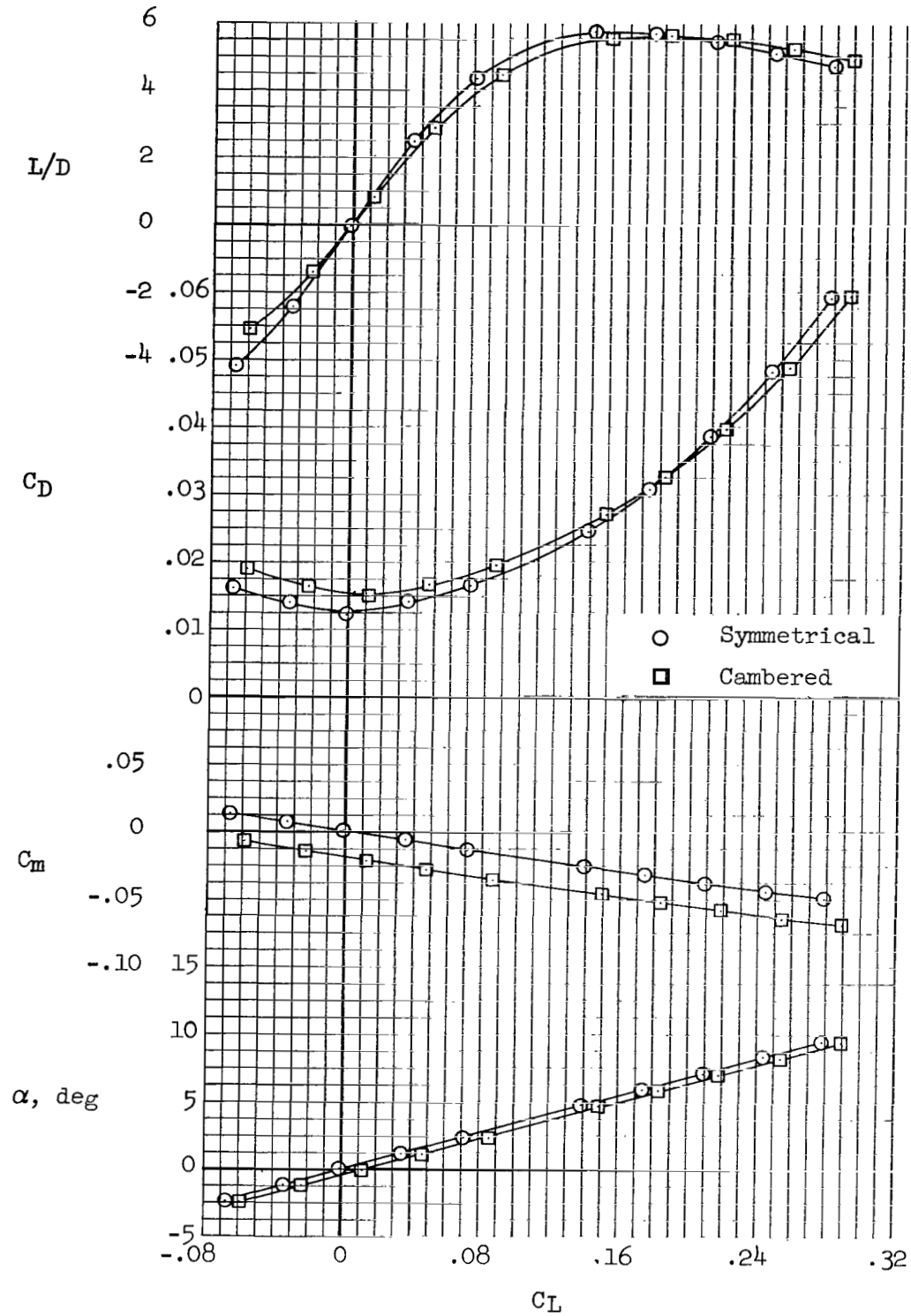

(a) M = 1.99

Figure 4.- Longitudinal aerodynamic characteristics of the model with a symmetrical and a cambered wing.

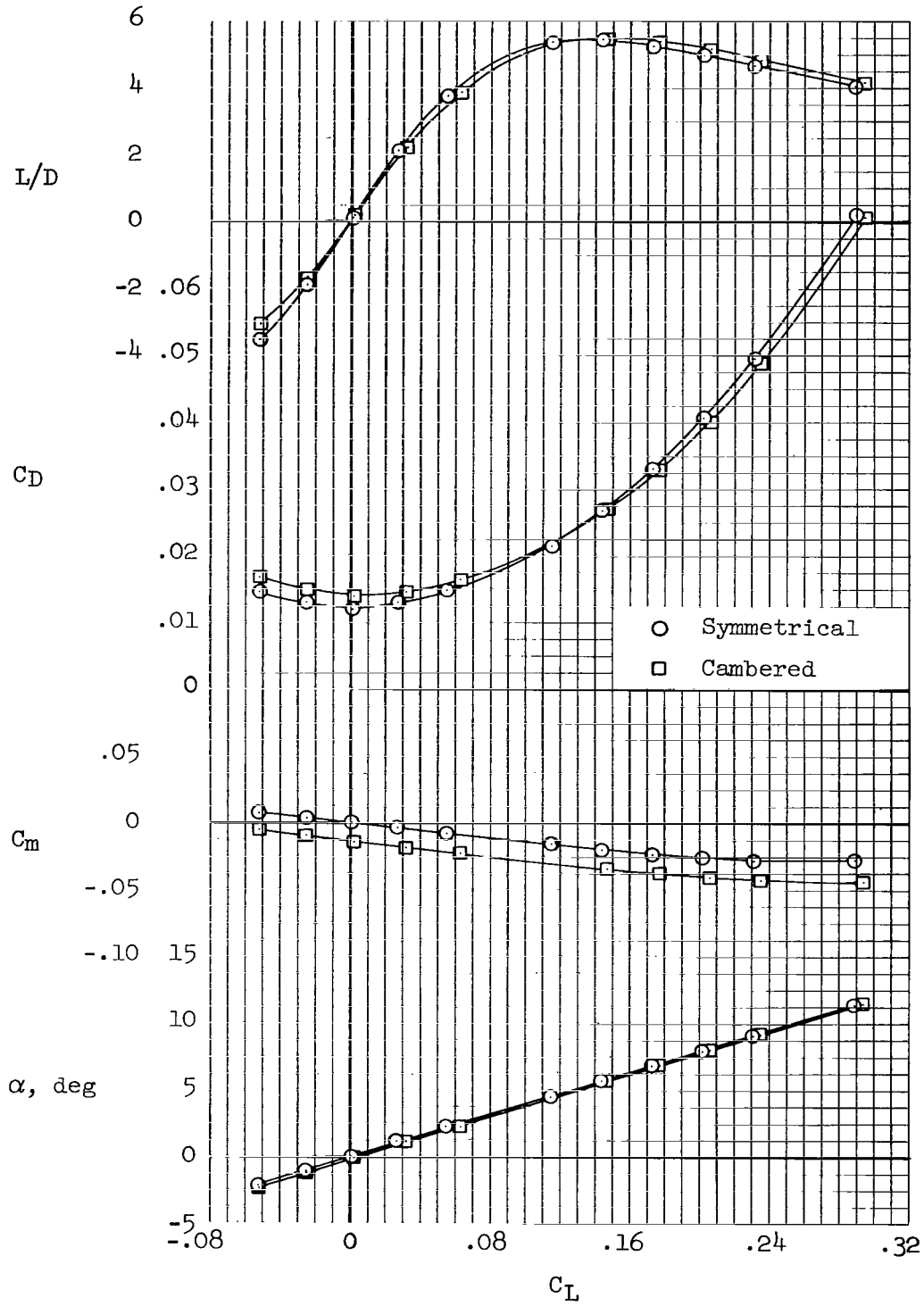

(b) M = 2.56

Figure 4.- Continued.

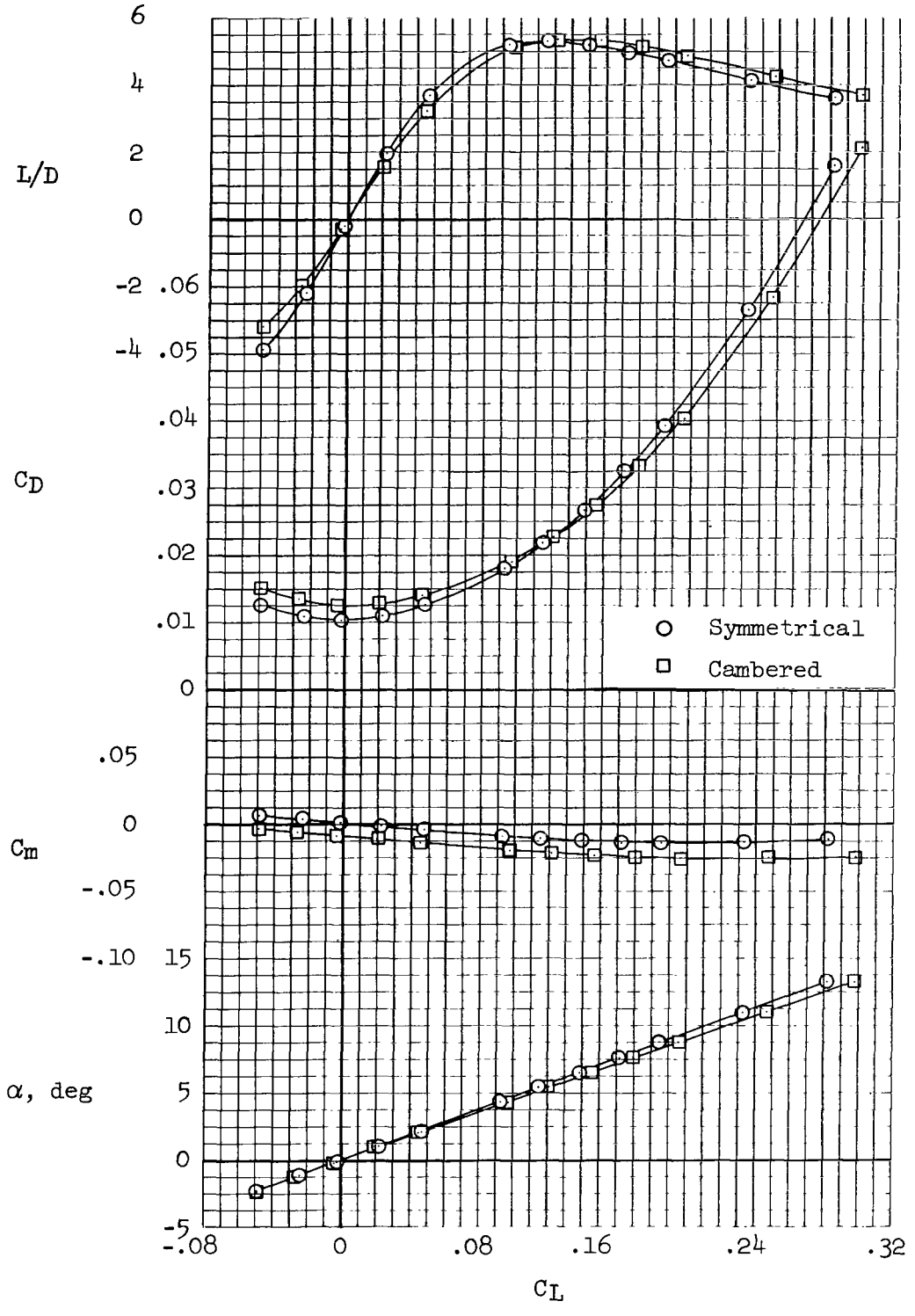

(c) M = 3.14

Figure 4.- Continued.

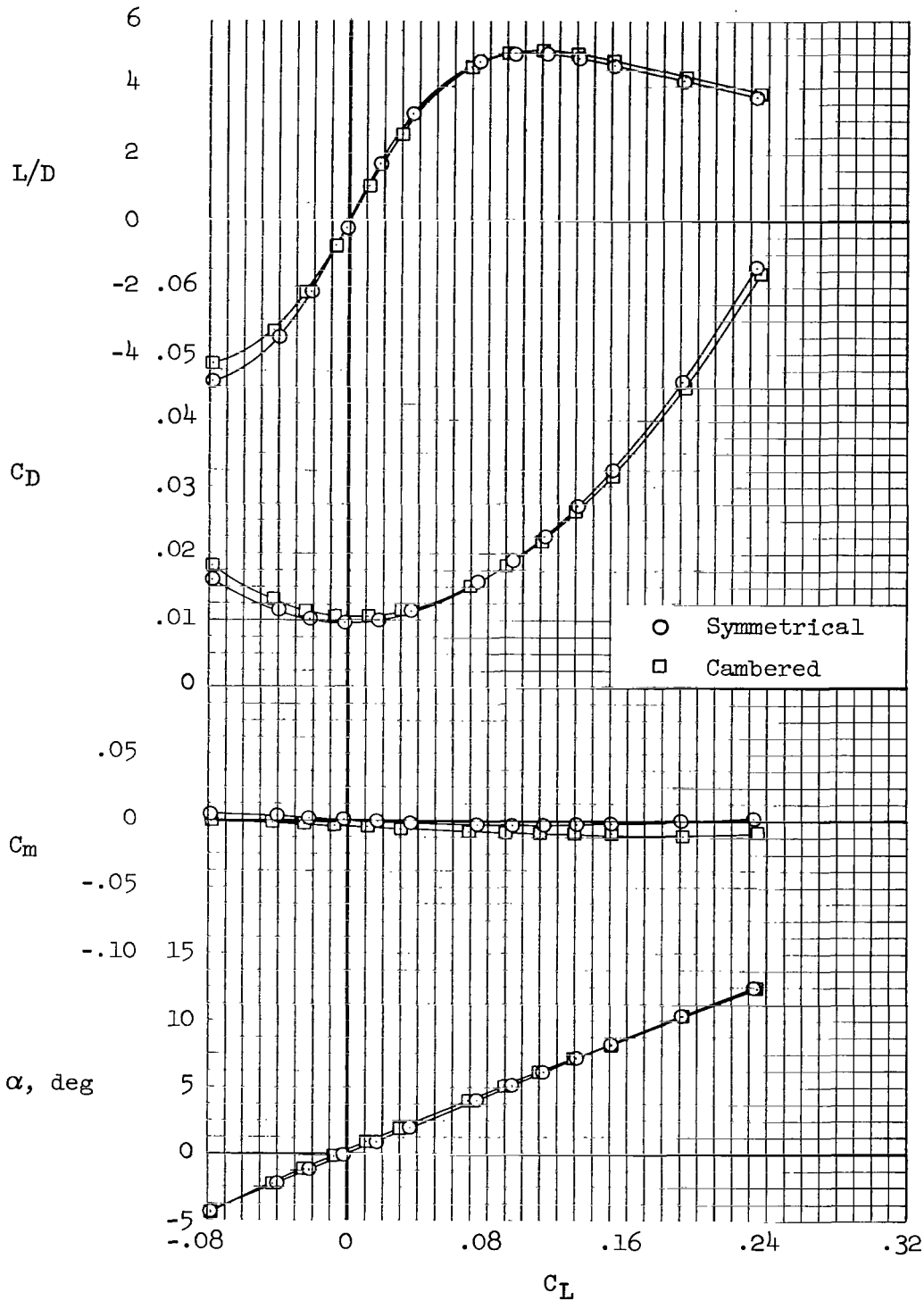

(d) M = 4.07

Figure 4.- Continued.

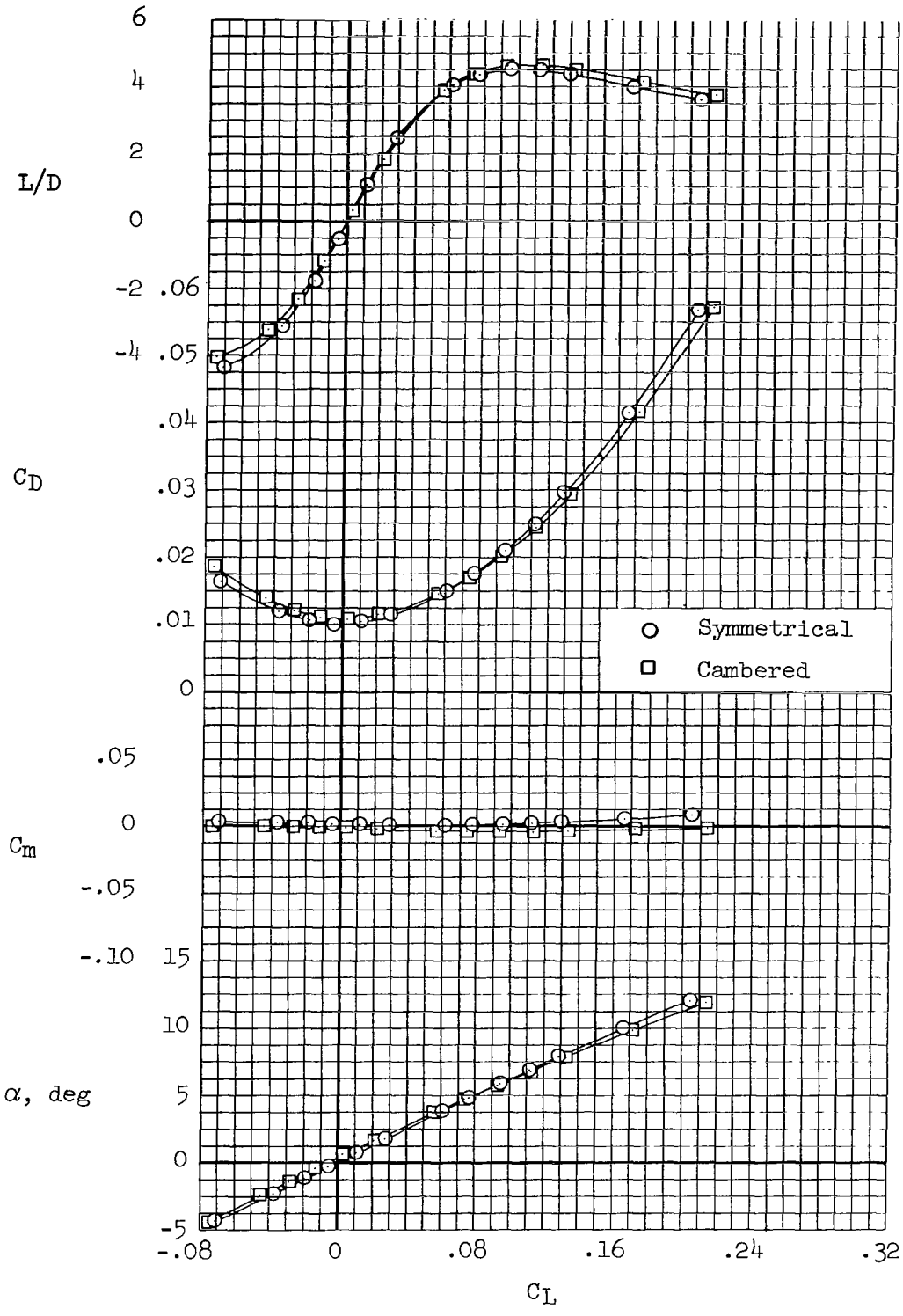

(e) M = 4.81

Figure 4.- Continued.

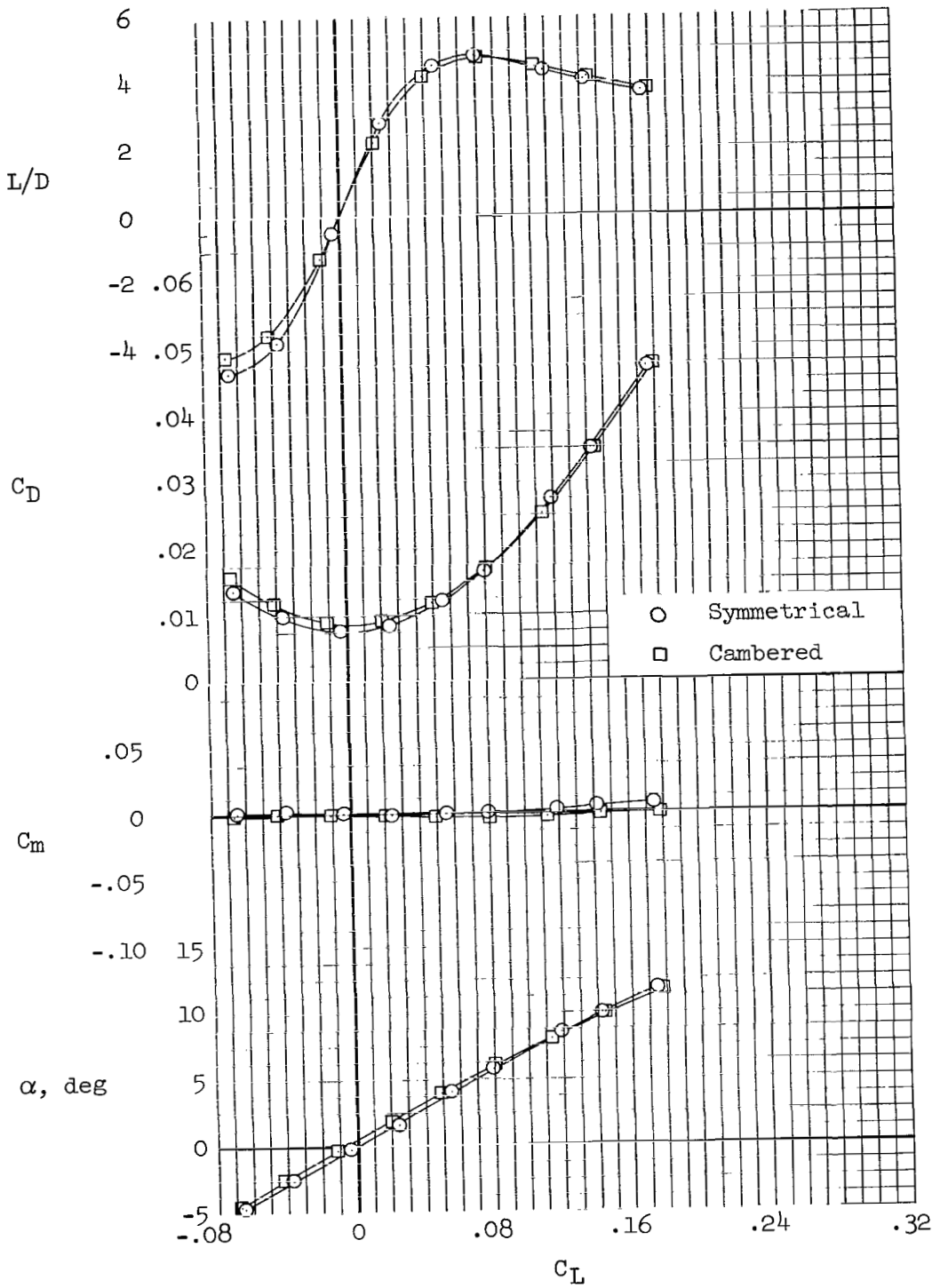

(f) M = 5.31

Figure 4.- Continued.

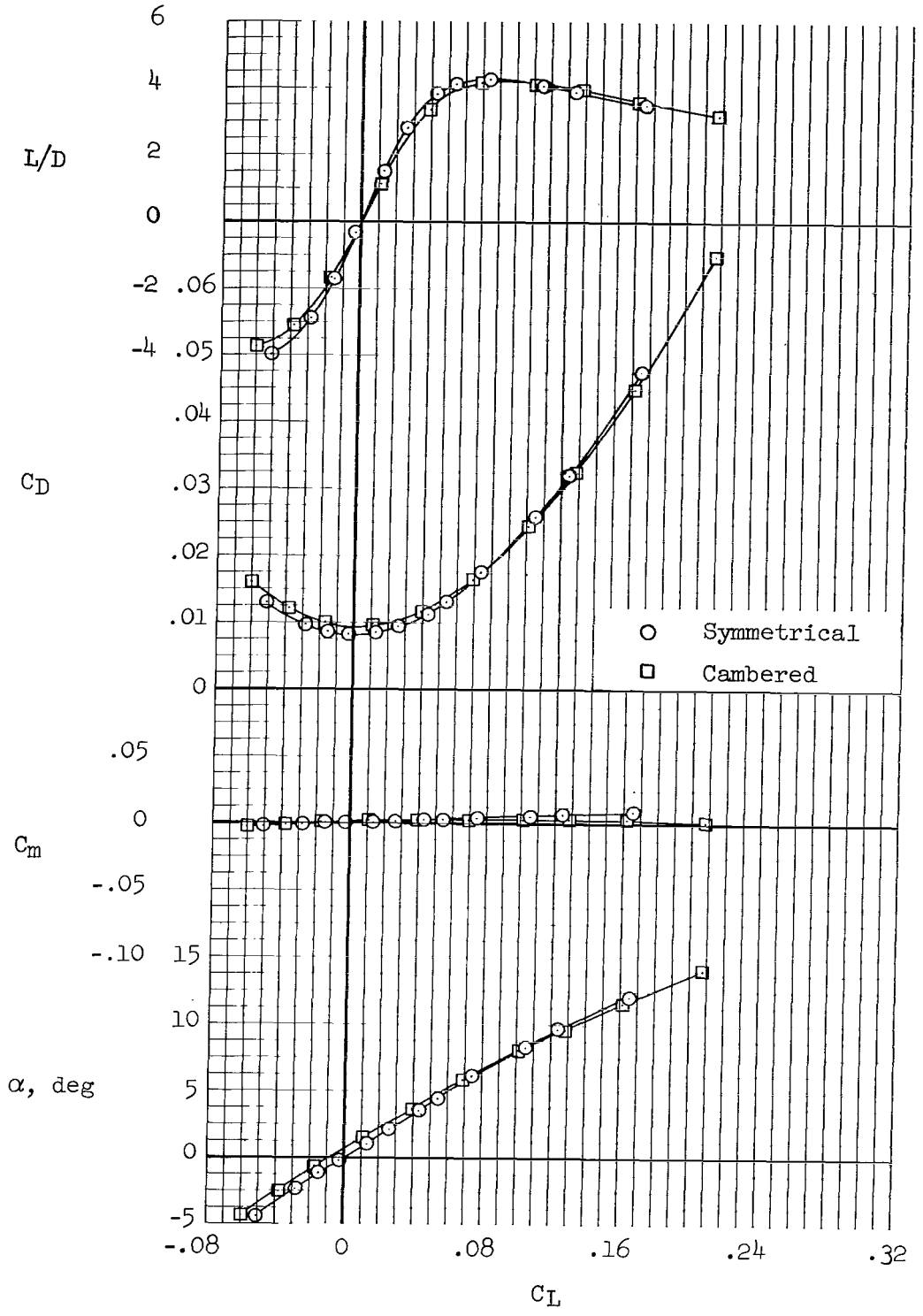

(g) M = 7.42

Figure 4.- Continued.

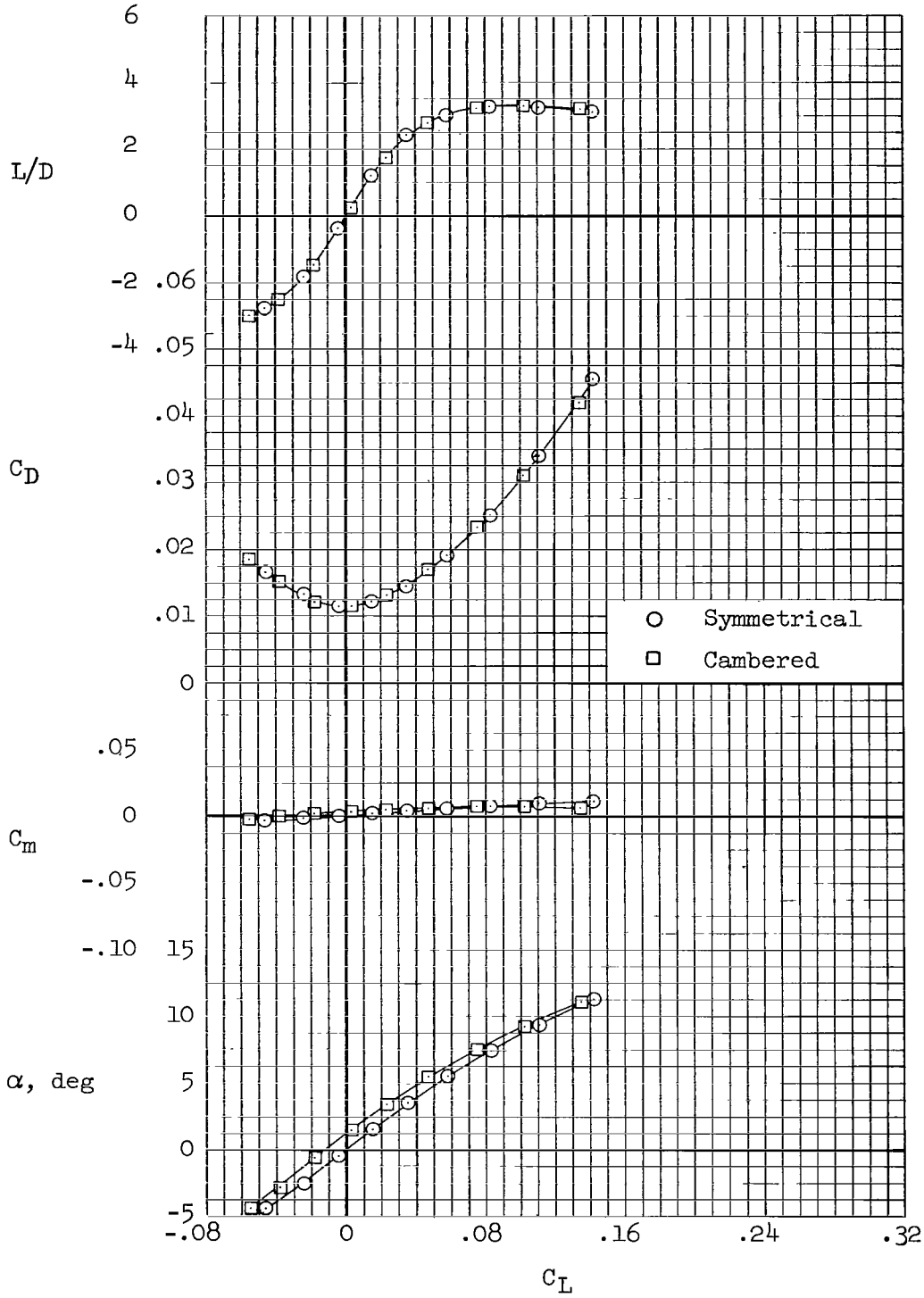

(h) M = 10.70

Figure 4.- Concluded.

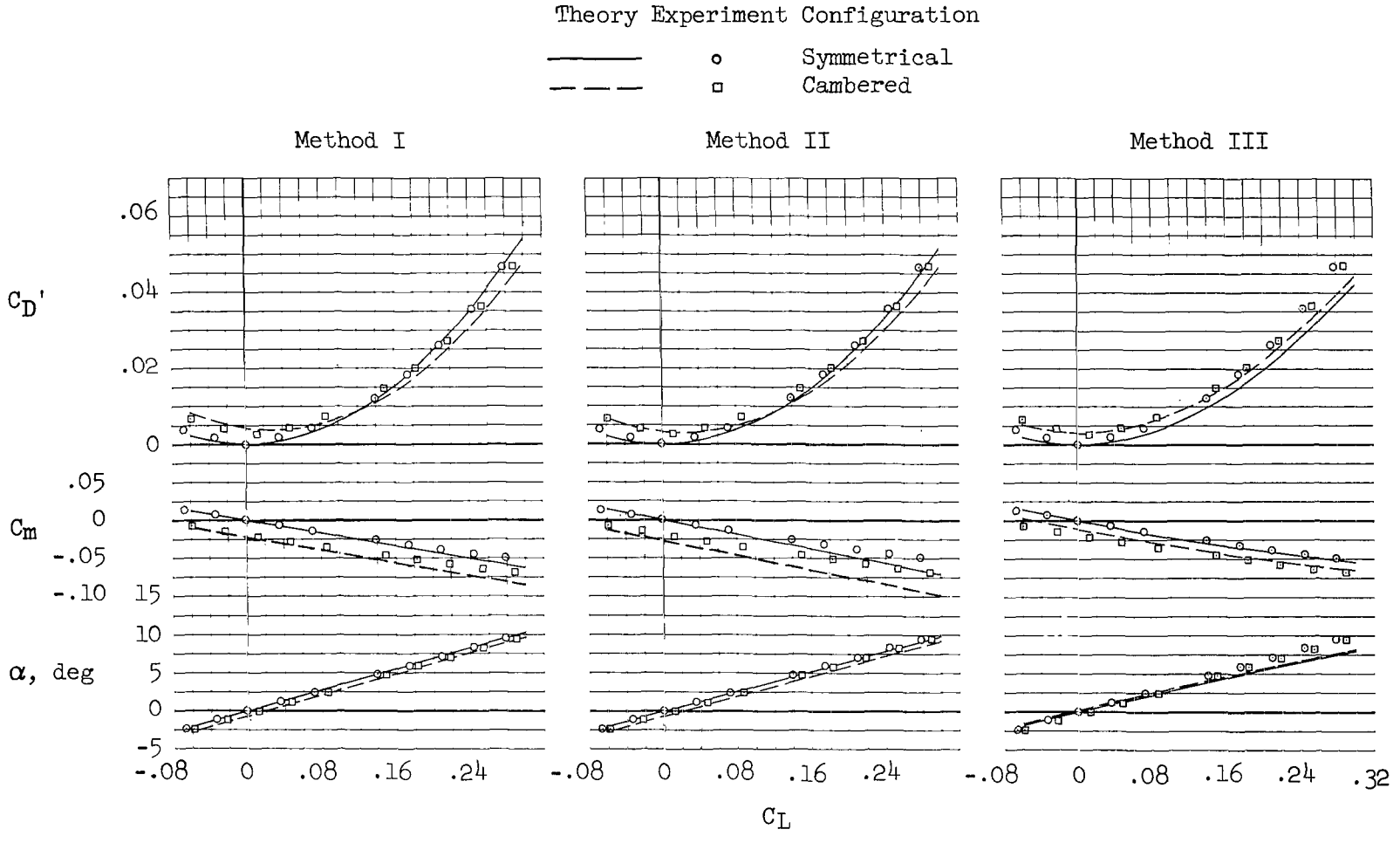

(a) M = 1.99

Figure 5.- Experimental and theoretical aerodynamic characteristics of the model with a symmetrical and a cambered wing.

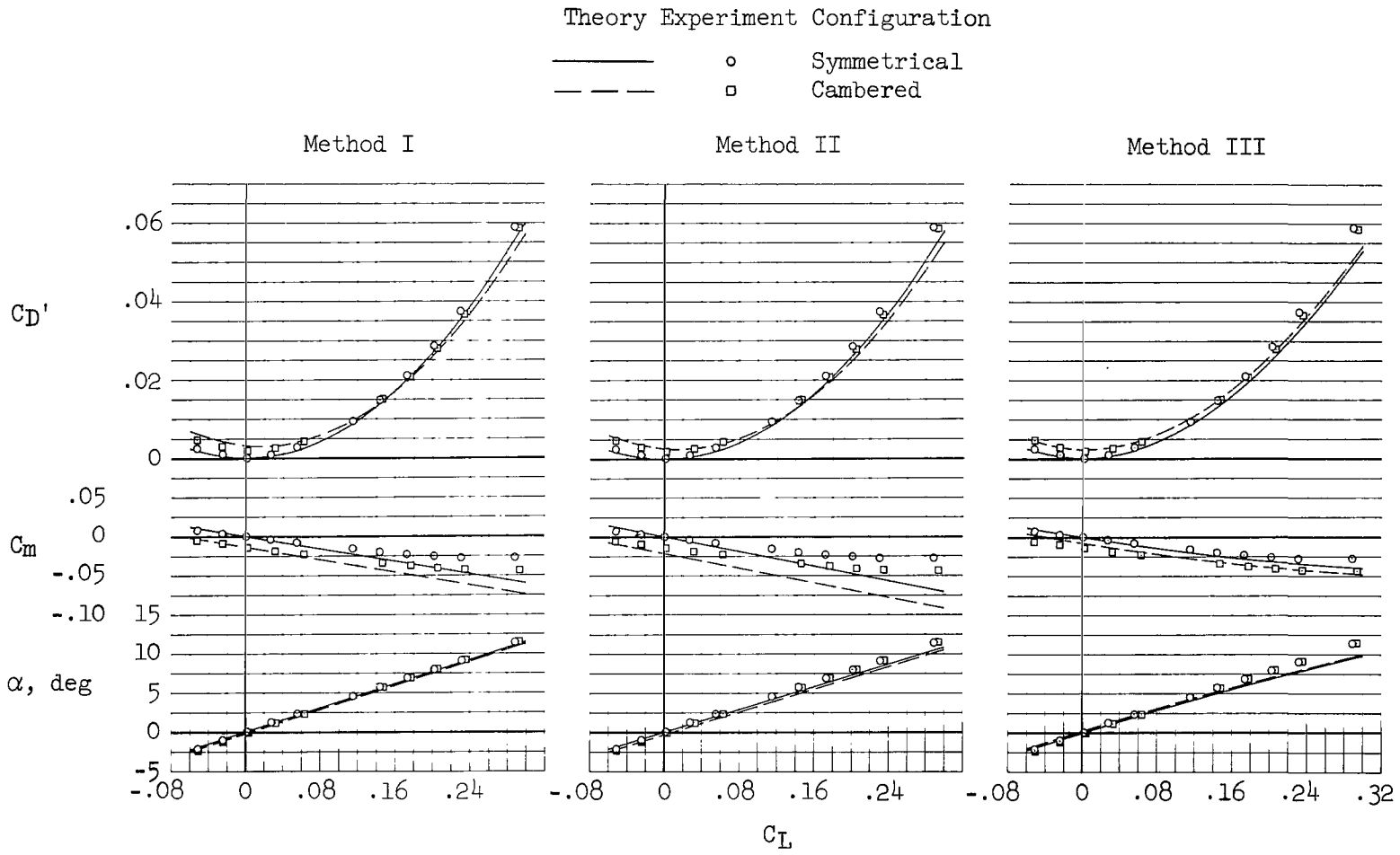

(b) M = 2.56

Figure 5.- Continued.

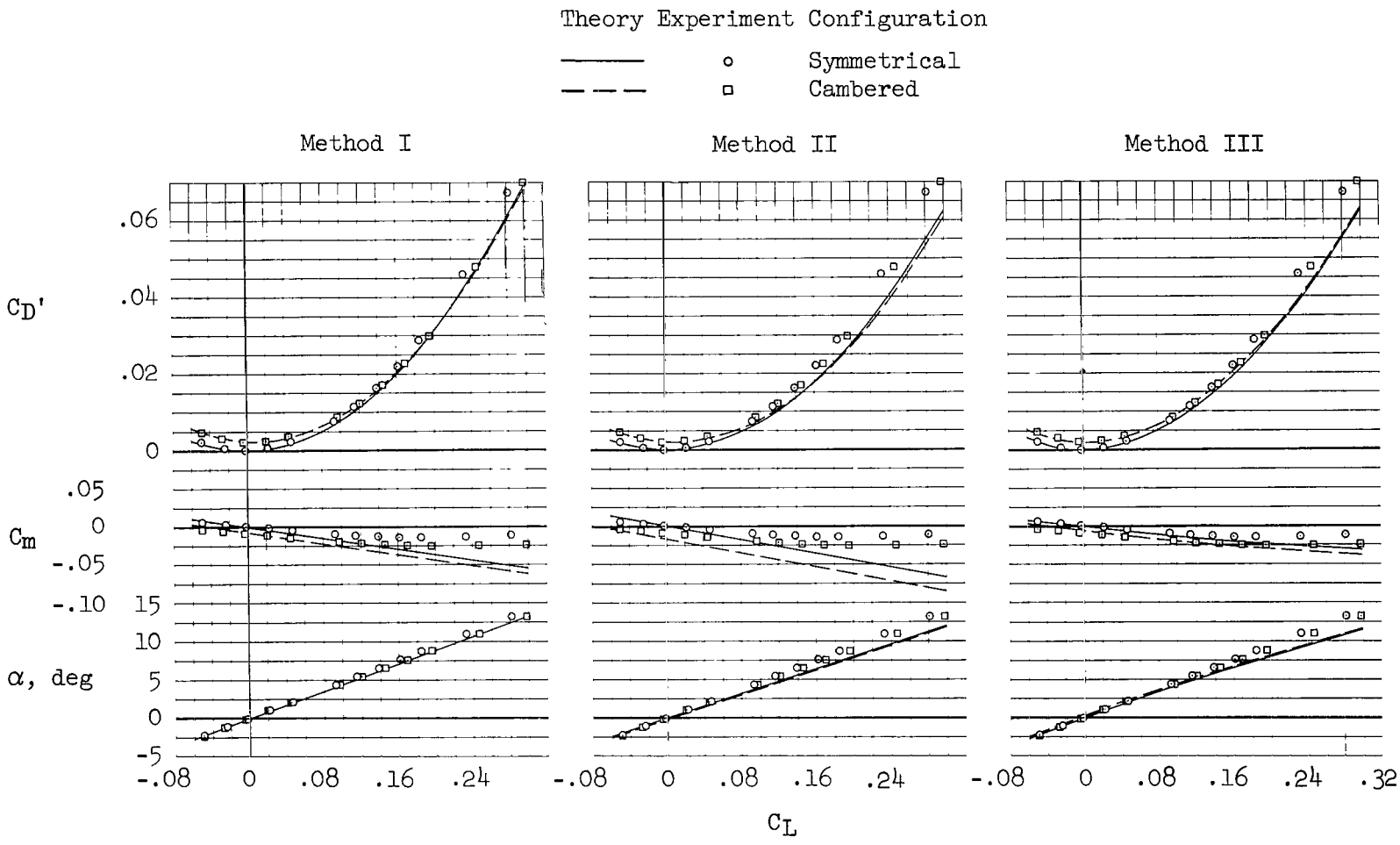

(c) M = 3.14

Figure 5.- Continued.

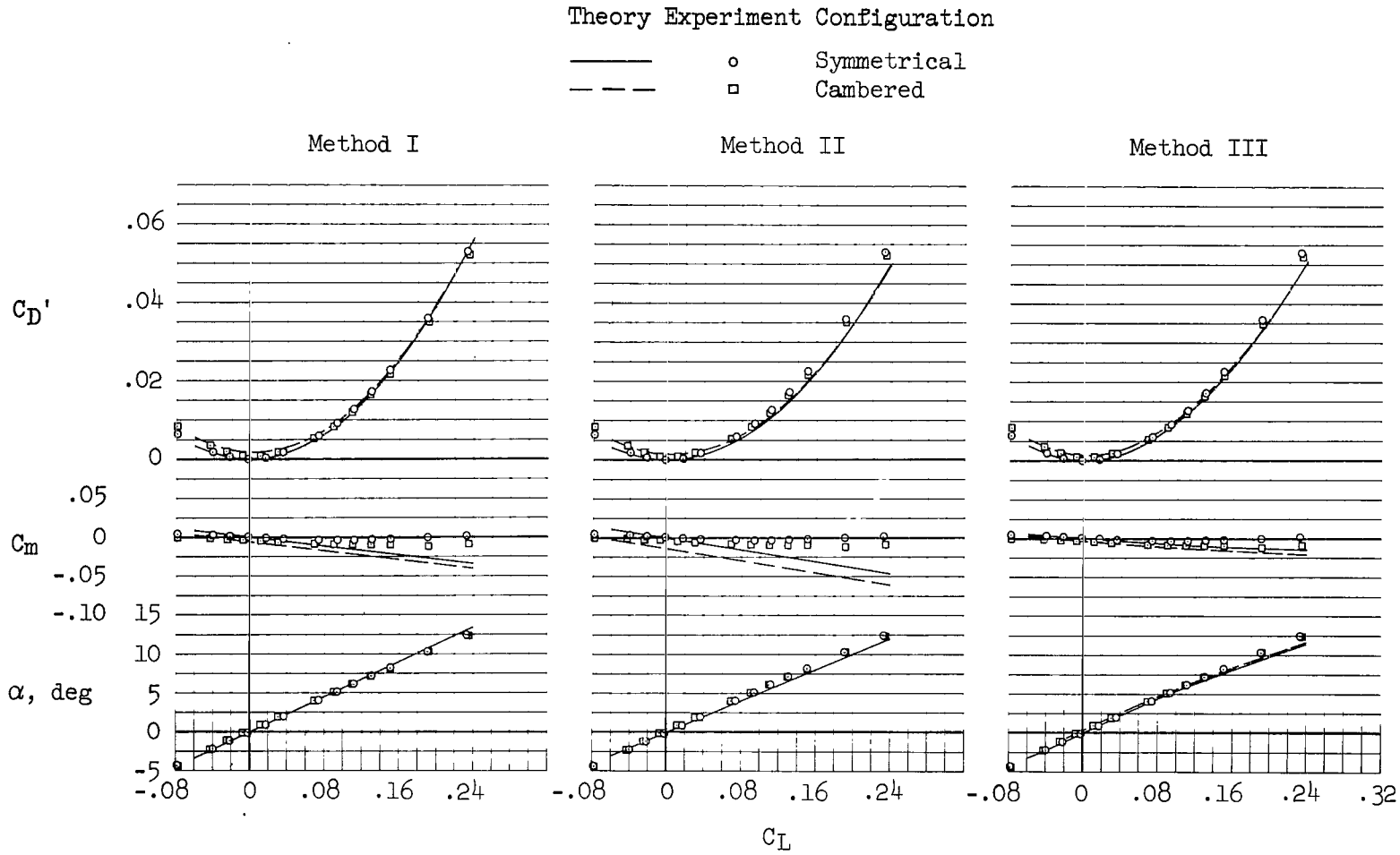

(d) M = 4.07

Figure 5.- Continued.

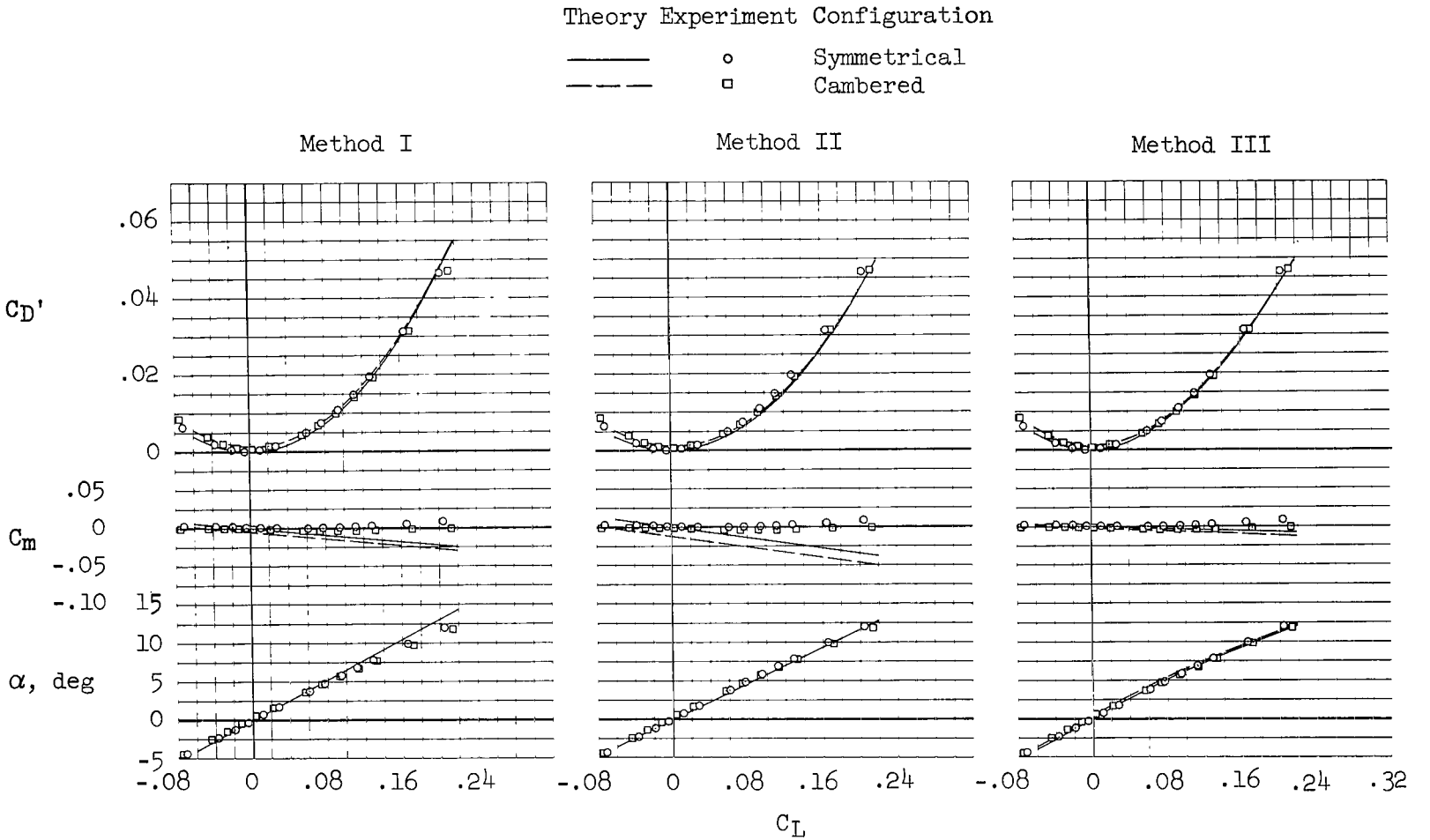

(e) M = 4.81

Figure 5.- Continued.

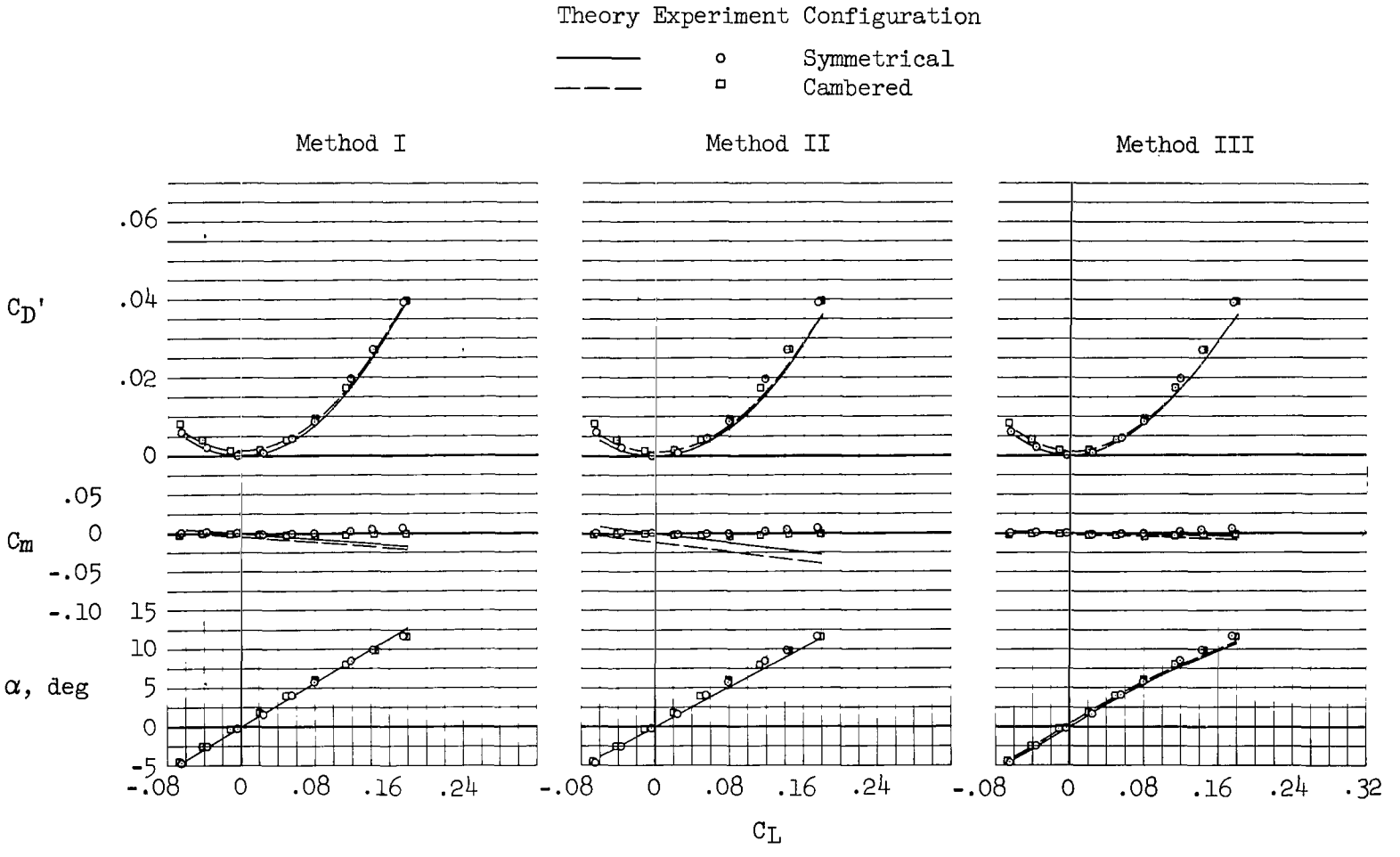

(f) M = 5.31

Figure 5.- Continued.

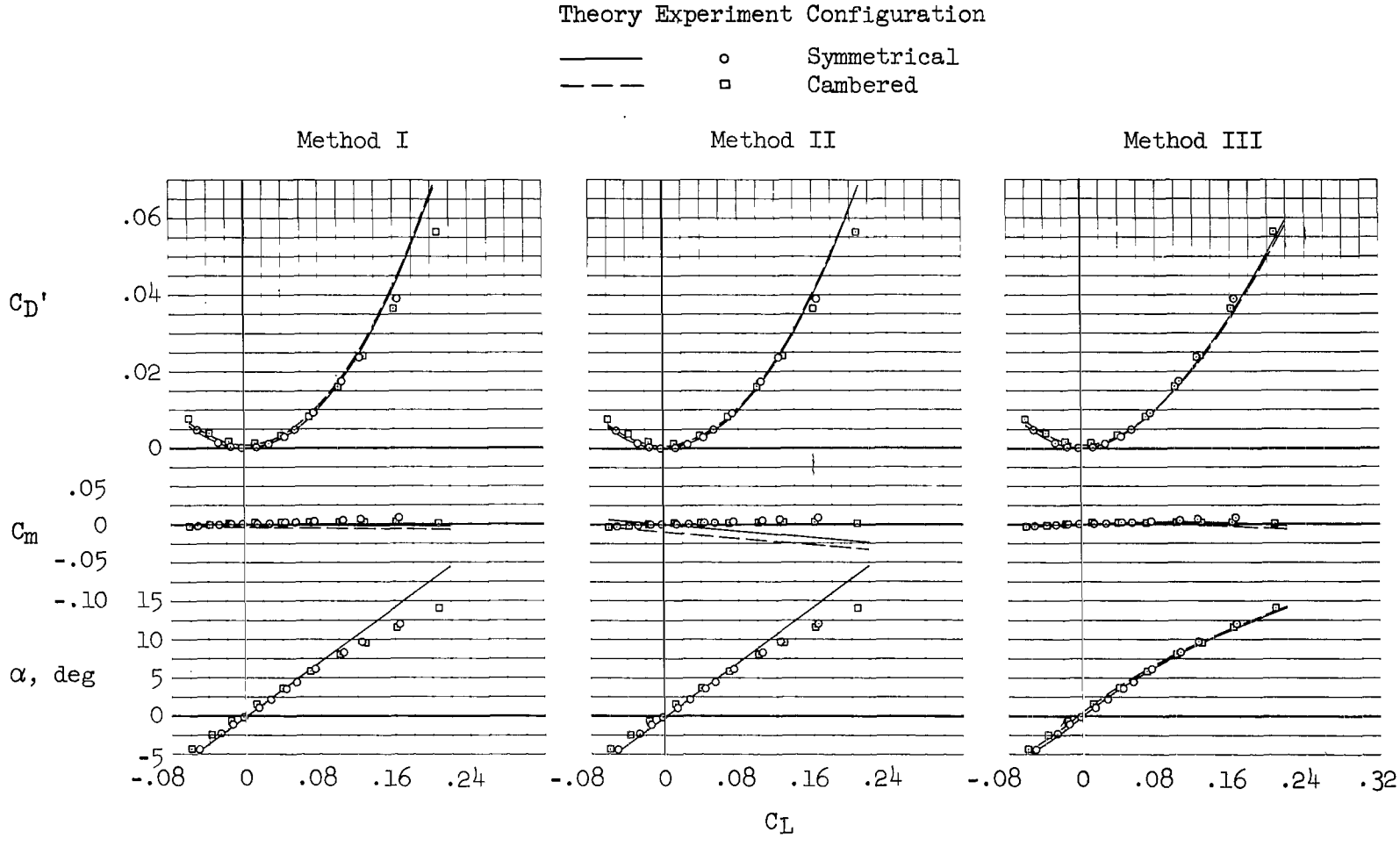

(g) M = 7.42

Figure 5.- Continued.

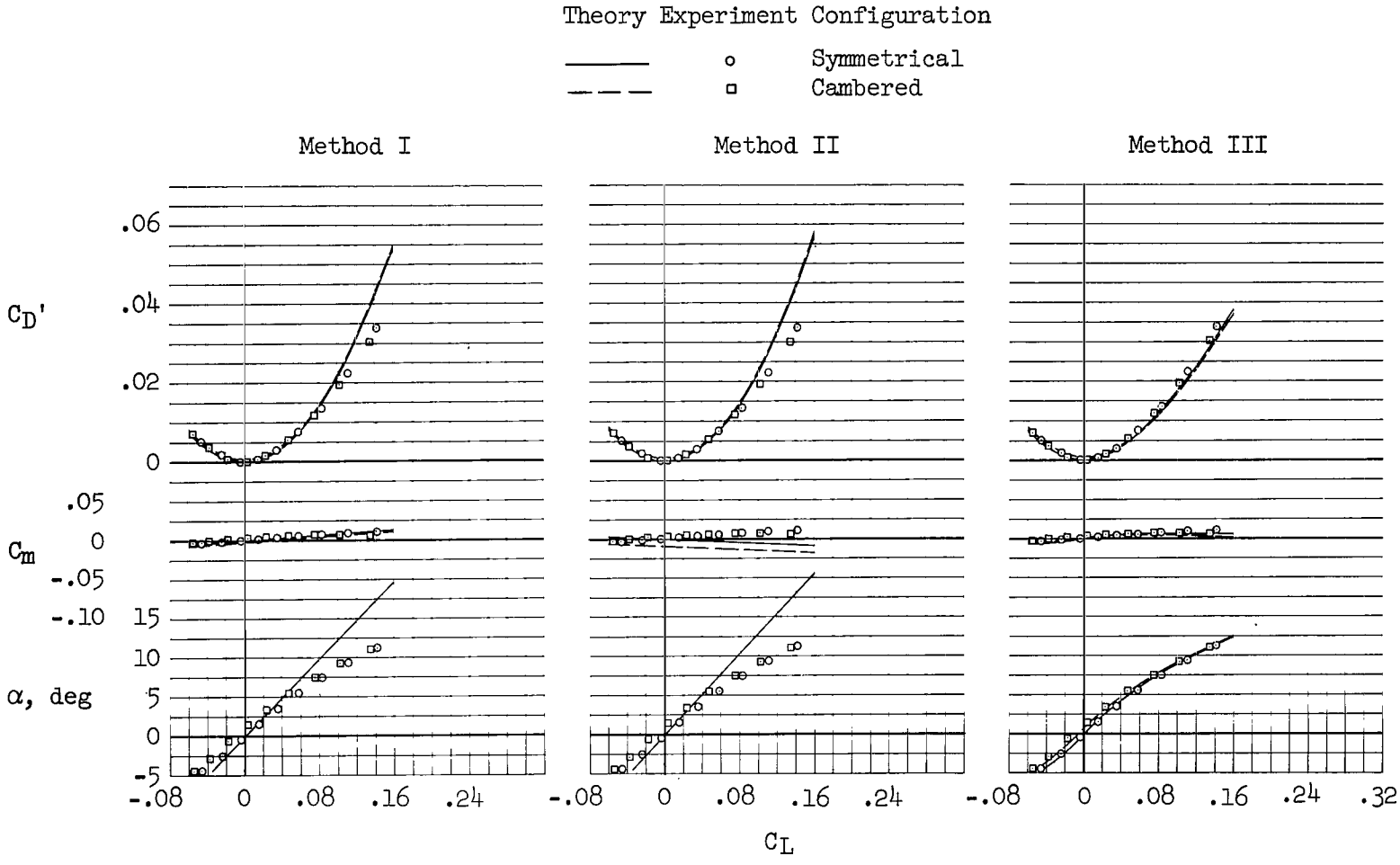

(h) M = 10.70

Figure 5.- Concluded.

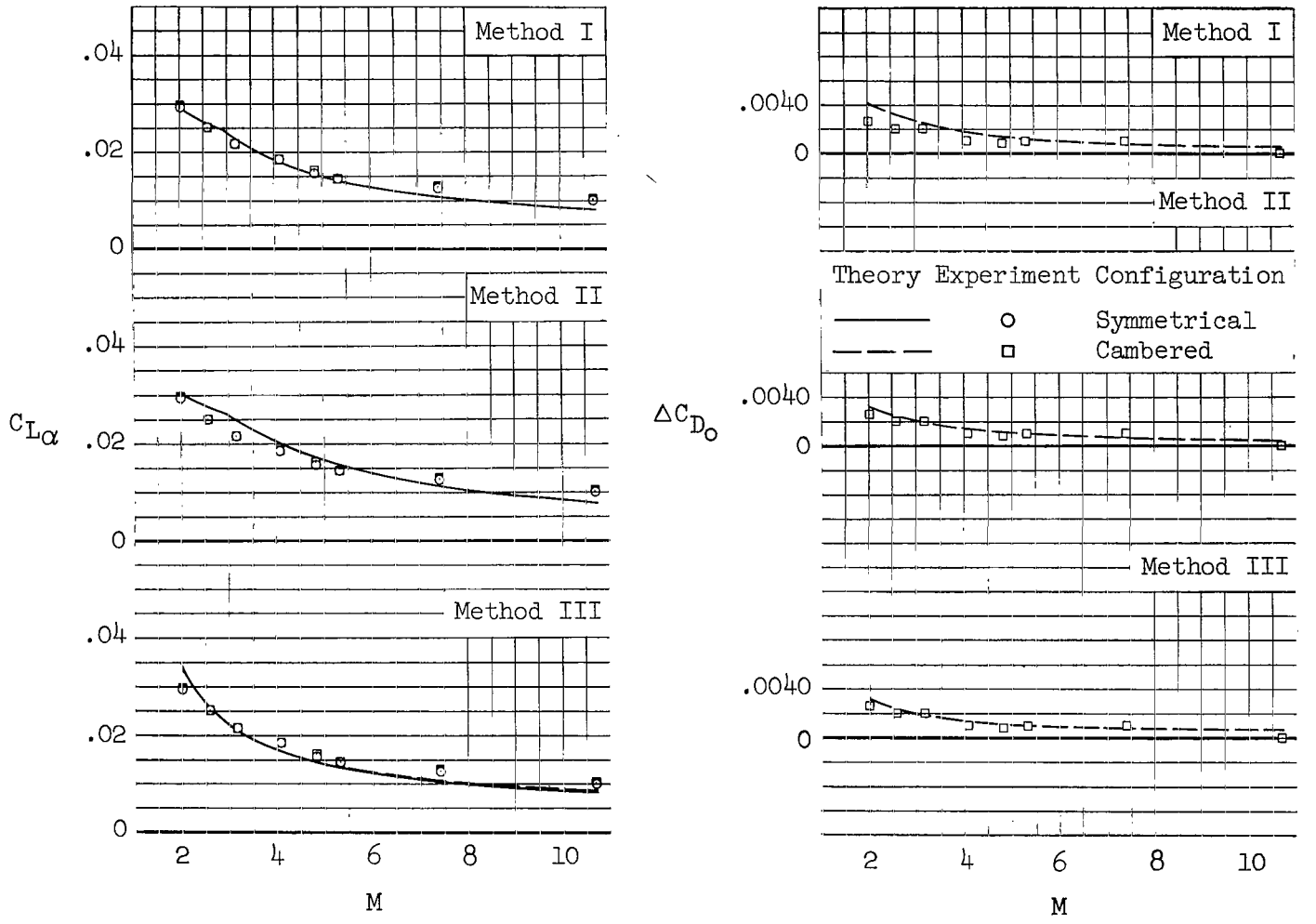

(a) Lift-curve slope and incremental drag at zero lift.

Figure 6.- Summary of experimental and theoretical aerodynamic characteristics of the model with a symmetrical and a cambered wing as a function of Mach number.

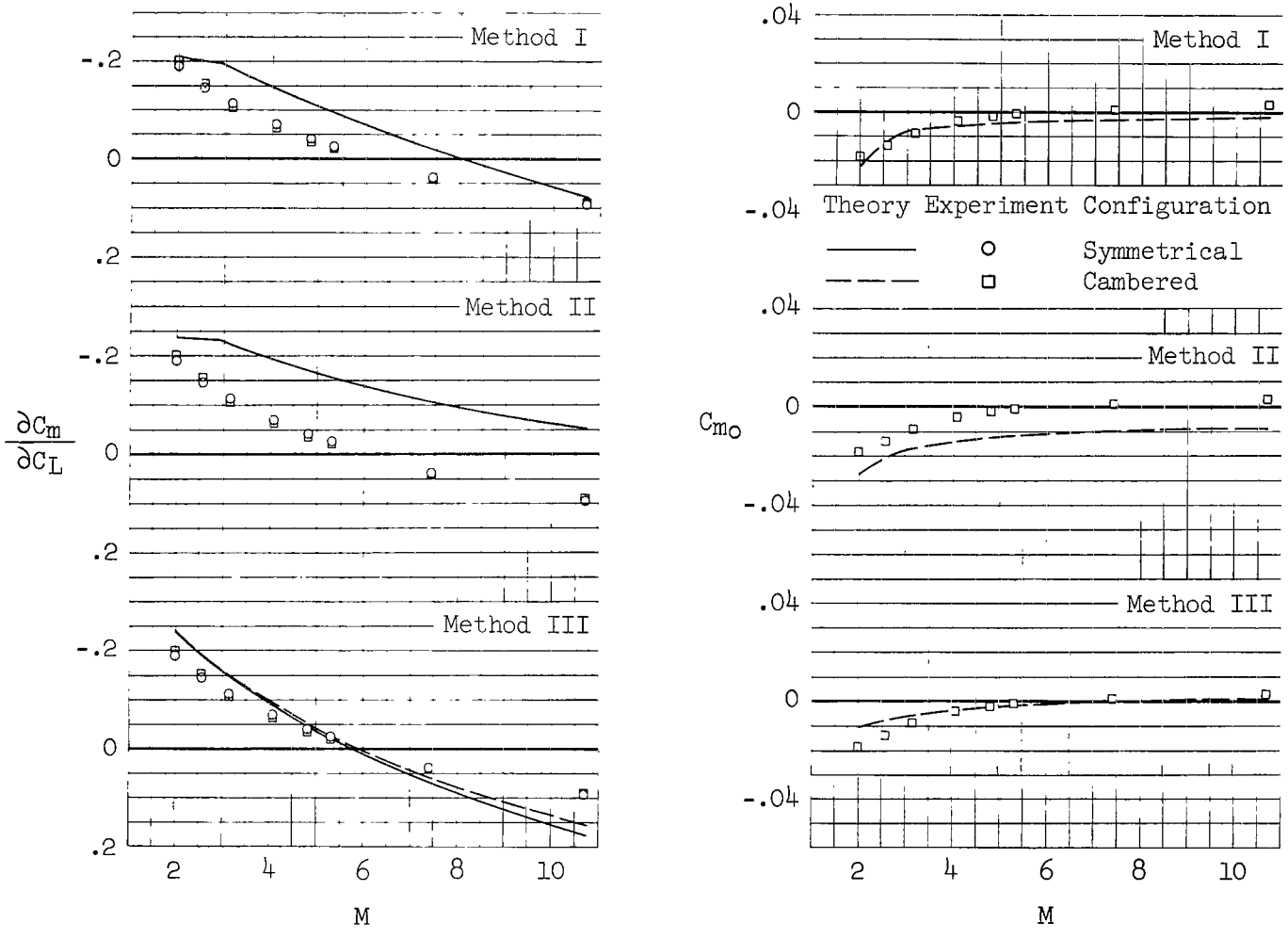

(b) Pitching-moment characteristics

Figure 6.- Concluded.

"The aeronautical and space activities of the United States shall be conducted so as to contribute . . . to the expansion of human knowledge of phenomena in the atmosphere and space. The Administration shall provide for the widest practicable and appropriate dissemination of information concerning its activities and the results thereof."

—NATIONAL AERONAUTICS AND SPACE ACT OF 1958

NASA SCIENTIFIC AND TECHNICAL PUBLICATIONS

TECHNICAL REPORTS: Scientific and technical information considered important, complete, and a lasting contribution to existing knowledge.

TECHNICAL NOTES: Information less broad in scope but nevertheless of importance as a contribution to existing knowledge.

TECHNICAL MEMORANDUMS: Information receiving limited distribution because of preliminary data, security classification, or other reasons.

CONTRACTOR REPORTS: Scientific and technical information generated under a NASA contract or grant and considered an important contribution to existing knowledge.

TECHNICAL TRANSLATIONS: Information published in a foreign language considered to merit NASA distribution in English.

SPECIAL PUBLICATIONS: Information derived from or of value to NASA activities. Publications include conference proceedings, monographs, data compilations, handbooks, sourcebooks, and special bibliographies.

TECHNOLOGY UTILIZATION PUBLICATIONS: Information on technology used by NASA that may be of particular interest in commercial and other non-aerospace applications. Publications include Tech Briefs, Technology Utilization Reports and Notes, and Technology Surveys.

Details on the availability of these publications may be obtained from:

SCIENTIFIC AND TECHNICAL INFORMATION DIVISION

NATIONAL AERONAUTICS AND SPACE ADMINISTRATION

Washington, D.C. 20546